Electron mobility in two coupled δ layers

Guo-Qiang Hai and Nelson Studart
Departamento de Física, Universidade Federal de São Carlos, 13565-905 São Carlos, São Paulo, Brazil

François M. Peeters
Department of Physics, University of Antwerp (UIA), B-2610, Antwerpen, Belgium
(Received 4 May 1995; revised manuscript received 6 July 1995)

The low-temperature transport properties are studied for electrons confined in δ-doped semiconductor structures with two sheets in parallel. The subband quantum mobility and transport mobility are calculated numerically for the Si δ-doped GaAs systems. The effect of coupling of the two δ layers on the electron transport is investigated. Our calculations are in good agreement with experimental results.

I. INTRODUCTION

In recent years, an appreciable amount of work has been devoted to the electron transport properties in δ-doped semiconductor systems.[1–13] The quasi-two-dimensional electron system in δ-doped semiconductors is realized, typically, by a very thin doped layer ($W_D \lesssim 20$ Å) of high doping concentration ($N_D \gtrsim 10^{12}$ cm^{-2}). On one hand, a high concentration of impurities leads to a high electron density in the system and several subbands are populated. On the other hand, as a consequence, this results in a very strong scattering on the electrons and, consequently, a low electron mobility. In order to fabricate high-mobility δ-doped devices, some works are focused in improving doping and material growth techniques.[2,4,5] An alternative way to improve the electron mobility in the δ-doped semiconductors, which has been proposed recently, is to make a structure with double δ layers.[10–13] It is expected that the coupling between the two layers leads to an increase of the average distance of the electrons from the doped layers. The impurity scattering is then reduced and the electron mobility is enhanced. It was shown that the electron mobility is increased by two to five times over that of a single δ-doped case.[10]

In previous works,[7,8] we studied theoretically the electron transport properties in single δ-layer systems. The effects of the doping concentration, thickness of the doped layer, as well as the background acceptor concentration on the electron subband mobility were investigated. The screening of the electron gas on the impurity scattering potential was included within the static random-phase approximation (RPA). In this paper, we report a theoretical study of the electron transport properties in double δ layer systems. We calculate the electron subband mobility for two interacting Si δ-doped layers in GaAs based on the self-consistent calculation of the electronic structure and wave functions in such a system. The electron subband quantum and transport mobilities are determined from the different scattering times connected to the average time between the scattering events. The quantum lifetime or the single particle relaxation time is the averaged elastic scattering time. On the other hand, in order to obtain the transport lifetime or the momentum relaxation time, every scattering event is averaged over its projection of the outgoing wave vector on the incident direction.[2] For a discussion from a theoretical point of view, see Ref. 14. Experimentally, the quantum mobility is obtained by Shubnikov–de Haas (SdH) measurements and the transport mobility is determined by the so-called mobility spectrum technique or by Hall measurements combined with the subband electron density obtained from SdH measurements.[2,11] We show the effect of the coupling between the two δ layers on the quantum and transport mobility of electrons in different subbands. In Sec. II, the self-consistent electronic structure of the coupled δ wells is determined and in Sec. III, the electron mobilities are numerically calculated and the theoretical results are compared with the available experimental ones.

II. SELF-CONSISTENT ELECTRONIC STRUCTURE

We consider the Si δ-doped GaAs structure with doubly doped layers in parallel. We assume that the two doped layers are symmetric, i.e., they have the same thickness and doping concentration. If we take the doped layers in the xy plane, the donor impurity distribution can be written as

$$n_D(z) = \begin{cases} N_D/W_D, & (W_S - W_D)/2 < |z| < (W_S + W_D)/2 \\ 0, & \text{otherwise}, \end{cases} \quad (1)$$

where N_D is the donor areal concentration of each layer, W_D the thickness of the doped layer, and W_S the separation between the two layers. In Eq. (1), we have assumed $W_S > W_D$. For $W_S \leq W_D$, the two doped layers become overlapped. In this case, we deal with the system as single doped layer.[7] The electron energy and wave function in the system can be written as $E_n(\vec{k}_\parallel) = E_n + \varepsilon(\vec{k}_\parallel)$, where n =1, 2, 3,... is the subband index, $\varepsilon(\vec{k}_\parallel) = \hbar^2 k_\parallel^2/2m^*$ is the electron kinetic energy, and $\vec{k}_\parallel$ the electron wave vector in the plane. The subband energies E_n and wave functions $\psi_n(z)$ are obtained from the self-consistent solution of the coupled one-dimensional Schrödinger and Poisson equations. In the calculation, we assume that all the impurities in the doping layers are ionized and the conduction band is parabolic. We took the parameters $m^* = 0.067m_e$, $\epsilon_0 = 13.18$, and the energy gap of GaAs $E_g = 1.52$ eV. The exchange-correlation potential of the electron gas was included within the local-density approximation.[15,7,8] In Fig. 1, the effective confinement potential $V_{sc}(z)$, the subband energies, and the probability distributions of the electrons in different subbands are depicted in the case of a structure with $W_S = 160$ Å, $W_D = 10$ Å, $N_D = 2.5 \times 10^{12}/\text{cm}^2$, and background acceptor concentration $n_A = 10^{15}/\text{cm}^3$. The shadow indicates the impurity sheets. In this figure $V_{sc}(z)$ is given by the thick curve and the thin curves indicate the subband electron distributions. It is seen that the lowest two levels are closed to each other and their respective electron distributions, which strongly overlap with the impurity layers, are very similar. Furthermore, the electron wave functions in the higher levels spread out in a much wider region as compared with those of the lowest subbands. Notice that the wave functions of the lowest two subbands have different parity. One ($n = 1$) is symmetric and the other one ($n = 2$) is antisymmetric. In the case of $E_1 = E_2$, the two levels become degenerate and the wave function can also be expressed as $\psi_\pm(z) = [\psi_1(z) \pm \psi_2(z)]/\sqrt{2}$, where $\psi_+(z)$ and $\psi_-(z)$ present the electron states in the right and the left quantum well, respectively. In Fig. 2, the subband energy E_n is depicted as a function of the separation of the two sheets W_S for $N_D = 2.5 \times 10^{12}/\text{cm}^2$, $W_D = 10$ Å, and $n_A = 10^{15}/\text{cm}^3$. The dashed curve presents the barrier (at $z = 0$) between the two quantum wells. For small W_S, where the barrier $V_{sc}(0)$ is much smaller than the lowest subband energy, the system is similar to the single δ layer. When $W_S \leq W_D$, the system becomes a single doped layer with doping concentration $2N_D$. With increasing W_S, the barrier $V_{sc}(0)$ increases rapidly. We find that $E_1 = V_{sc}(0)$ at $W_S = 89.4$ Å, and $E_2 = V_{sc}(0)$ at $W_S = 132.5$ Å. For $W_S = 200$ Å, the first two subbands become almost degenerate. At small W_S, the lowest three subbands are populated by electrons. The $n = 4$ and 5 subbands become populated for $W_S \geq 46$ Å and 196 Å, respectively. When $W_S \to \infty$, the system behaves like two independent single δ layers and the energy level E_3 corresponds to the second level of the independent δ layer.

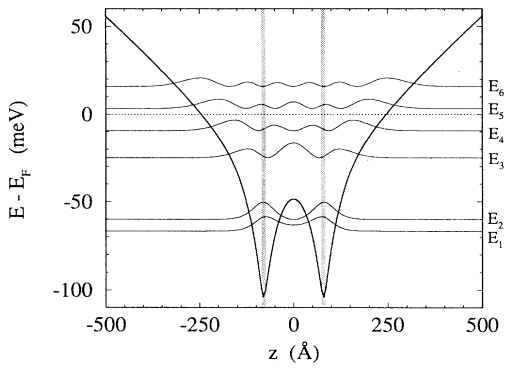

FIG. 1. The results of the self-consistent calculation of the effective confinement potential (thick-solid curve), the energy levels E_n, and the electron probability distribution (thin-solid curves) for a double δ layer structure of $W_S = 160$ Å, $W_D = 10$ Å, $N_D = 2.5 \times 10^{12}/\text{cm}^2$ for each layer, and $n_A = 10^{15}/\text{cm}^3$. The energy is measured from the Fermi energy (thin-dotted line), and the shadow indicates the Si δ-doped layers.

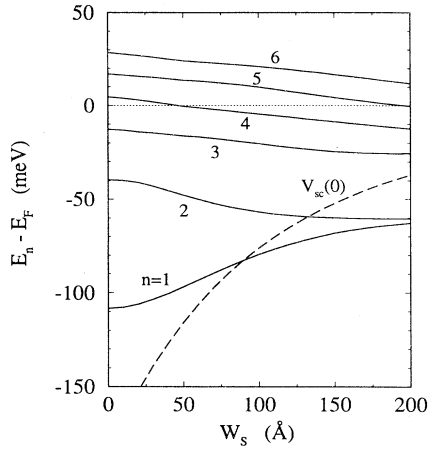

FIG. 2. The subband energy as a function of the separation between the two doped layers with $N_D = 2.5 \times 10^{12}/\text{cm}^2$ and $W_D = 10$ Å for each layer. The dash curve indicates the barrier at $z = 0$ between the two coupled quantum wells. $n_A = 10^{15}/\text{cm}^3$.

III. ELECTRON MOBILITIES

Based on the above self-consistent solution of the electronic structure and the wave functions, we study the electron transport properties of the system. In the calculation, only the scattering by ionized donors in the doped layers are considered, because it is the most important scattering mechanism at low temperature. We consider the Coulomb scattering potential due to ionized impurities, distributed randomly in the doped layer at positions $\vec{R}_i$, whose two-dimensional Fourier transform is given by

$$v(q_\parallel, z) = -\frac{2\pi e^2}{\epsilon_0 q_\parallel} \sum_i e^{-q_\parallel |z - z_i|} e^{i\vec{q}_\parallel \cdot \vec{R}_{\parallel i}}. \quad (2)$$

Using the Fermi golden rule, the electron transition probability from state $|n,\vec{k}_\parallel\rangle$ to $|n',\vec{k}'_\parallel\rangle$ for the electron-impurity scattering is given by

$$W_{n,n'}(\vec{k}_\parallel,\vec{k}'_\parallel)=\frac{2\pi}{\hbar}|u_{n,n'}(\vec{q}_\parallel)|^2\delta_{\vec{k}'_\parallel-\vec{k}_\parallel,\vec{q}_\parallel}\delta[E_{n'}(k'_\parallel)-E_n(k_\parallel)], \tag{3}$$

where $u_{n,n'}(\vec{q}_\parallel)$ is the transition matrix element. Because of the high electron density in the present system, the screening effects of the electron gas on the scattering potential has to be taken into account properly. The screened ionized impurity potential can be obtained in terms of the static dielectric response function within the RPA.[7,16–19] The dielectric function in the present multisubband system has a tensor character given by $\epsilon_{nn',mm'}(\vec{q}_\parallel)$. For the present double δ layer system, the transition matrix elements, due to the screened scattering potential, is written as

$$|u_{n,n'}(\vec{q}_\parallel)|^2=\left(\frac{2\pi e^2}{\epsilon_0 q_\parallel}\right)^2\frac{N_D}{W_D}\int_{(W_S-W_D)/2}^{(W_S+W_D)/2}\times dz_i\{|G^+_{nn'}(q_\parallel,z_i)|^2+|G^-_{nn'}(q_\parallel,z_i)|^2\}, \tag{4a}$$

where

$$G^\pm_{n,n'}(q_\parallel,z_i)=\sum_{mm'}(\pm1)^{m+m'}\epsilon^{-1}_{nn',mm'}(\vec{q}_\parallel)G^{(0)}_{mm'}(q_\parallel,z_i), \tag{4b}$$

where the overlapping function $G^{(0)}_{n,n'}(q_\parallel,z_i)$ is written as

$$G^{(0)}_{n,n'}(q_\parallel,z_i)=\int_{-\infty}^{\infty}dz\psi_n(z)\psi_{n'}(z)e^{-q_\parallel|z-z_i|}, \tag{4c}$$

with the change in electron momentum, due to scattering given by

$$q_\parallel=\left[(E_n-E_{n'})\frac{2m^*}{\hbar^2}+2k_\parallel^2-2k_\parallel\cos\theta\sqrt{(E_n-E_{n'})\frac{2m^*}{\hbar^2}+k_\parallel^2}\right]^{1/2}, \tag{5}$$

and θ is the angle between $\vec{k}_\parallel$ and $\vec{k}'_\parallel$.

We have performed the numerical calculation for the electron subband transport and quantum mobility, using the self-consistent subband wave function to evaluate the transition matrix elements. In practical calculations, we have to limit the sum over (m,m') in Eq. (4b). For a system with N populated subbands, we include $N+2$ subbands in the matrix of the dielectric function, i.e., we consider all the occupied subbands and two empty ones. Within such an approximation, the dielectric function $\epsilon_{nn',mm'}(\vec{q}_\parallel)$ is approximated by an $(N+2)^2\times(N+2)^2$ matrix. The thick curves in Fig. 3 show the quantum mobility, as a function of W_S for $N_D=2.5\times10^{12}/\text{cm}^2$, $W_D=10$ Å, and $n_A=10^{15}/\text{cm}^3$. We found that the quantum mobility of the lowest subband μ_1^q increases slightly with increasing W_S until $W_S=130$ Å and then turns out to be a decreasing function. The μ_2^q decreases monotonously as a function of W_S. For small W_S, $\mu_2^q\gg\mu_1^q$. When $W_S>82$ Å, μ_2^q becomes smaller than μ_1^q and they are very close to each other. The mobility μ_3^q is about a factor of 3 larger than μ_1^q. μ_4^q is close to μ_3^q and it increases slowly with increasing W_S. At $W_S=46$ and 196 Å, due to the onset of the occupation of the subbands $n=4$ and 5, the calculated subband mobility exhibits an abrupt jump as a consequence of the intersubband interaction. We also notice that, at the onset of the occupation of $n=4$ subband, μ_1^q and μ_2^q have small decreasing jumps, due to the contribution of the intersubband scattering related to the $n=4$ subband. However, μ_3^q increases abruptly. Such a result reflects the screening effect in the intersubband interaction. At the onset of the occupation of $n=5$ subband, the changes of the quantum mobilities of the lower subbands are not pronounced. The experimental results of the quantum mobility[11] are presented by the different symbols in Fig. 3: circles ($n=1$), squares ($n=2$), triangles ($n=3$), and diamonds ($n=4$). Our calculation is in quite good agreement with the experimental results for the four subbands. The thick curves in Fig. 4 give the transport mobility as a function of W_S. It is seen that the subband transport mobility has a similar behavior as the quantum mobilities. But the transport mobilities of the lowest two subbands are about a factor 4 larger than the corresponding quantum mobilities. Such a factor is about 2–3 for the $n=3$ and 4 subbands. Besides, the transport mobility is different from the quantum mobility in the following ways. (i) $\mu_1^t\simeq\mu_2^t$ for $W_S>80$ Å, $\mu_2^t>\mu_3^t$ for $W_S<18$ Å, and $\mu_3^t\sim\mu_4^t$ for $W_S>150$ Å. (ii) At the onset of the occupation of the $n=4$ subband, μ_4^t is about a factor of 2 smaller than μ_3^t, but it increases rapidly and approaches to μ_3^t at larger W_S. (iii)

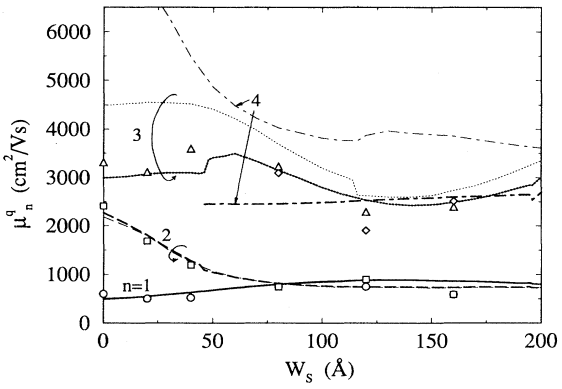

FIG. 3. The subband quantum mobility as a function of the separation of the two δ layers for $N_D=2.5\times10^{12}/\text{cm}^2$ and $W_D=10$ Å in Si δ-doped GaAs. The thick and thin curves indicate the calculation results of $n_A=10^{15}$ and 10^{14} cm^{-3}, respectively. The solid, dashed, dotted, and dotted-dashed curves present the results of the $n=1$, 2, 3, and 4 subbands, respectively. The experimental results are indicated by the circles, squares, triangles, and diamonds, which correspond to $n=1$, 2, 3, and 4, respectively (see Ref. 11).

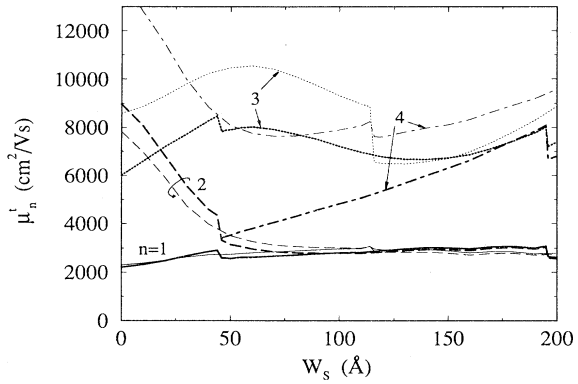

FIG. 4. The same as Fig. 3, but for the subband transport mobilities.

At the onset of the occupation of a higher subband, the transport mobilities of all the lower subbands exhibit an abrupt decrease. (iv) Intersubband scattering is stronger for the transport mobility. Unfortunately, as far as we know, there are no available low-temperature measurements of the transport mobility for our structure, except the experimental results for the Hall mobility for $T \geq 77$ K.[10]

We also examined the influence of the background acceptor concentration on the electron transport properties. The calculated quantum mobility and the transport mobility with $10^{14}/\text{cm}^3$ ($N_D = 2.5 \times 10^{12}/\text{cm}^2$ and $W_D = 10$ Å) are given in thin curves in Fig. 3 and Fig. 4, respectively. It is seen that n_A strongly influences the mobility of the electrons in the higher subbands in such a system. The mobilities of the $n = 3$ and 4 subbands are enhanced pronouncedly, due to the reduction of the background acceptor concentration. This is a rather indirect effect: the background acceptor concentration influences the band bending (e.g., higher concentration leads to a narrower confinement potential), which influences the distribution of electrons in real space and between the subbands (e.g., the conduction electrons become closer to the doped layers), and this in turn affects the mobility. We demonstrated explicitly this effect in the case of a single δ layer.[8]

In conclusion, we have presented a theoretical study of the electron subband mobility in double δ layer structures. The electron subband quantum and transport mobilities are calculated for the Si δ-doped GaAs systems. We found that, for $W_S \geq 50$ Å, the mobilities of the lowest two subbands are very close to each other and much smaller than those of the higher subbands. For $W_S \geq 120$ Å, the influence of the separation of the two doping layers on the subband quantum mobilities is not pronounced. Furthermore, the transport mobilities of the $n = 3$ and 4 subbands increase with increasing W_S. We also found that the background acceptor concentration modify the electron mobility of the higher subbands. Such an influence is very pronounced in the transport mobility. Our calculation of the electron quantum mobility is in good agreement with the experimental results of Refs. 11 and 2.

ACKNOWLEDGMENTS

This work was partially sponsored by the Conselho Nacional de Desenvolvimento Científico e Tecnológico (CNPq) and the Fundação de Amparo à Pesquisa do Estado de São Paulo (FAPESP). G.Q.H. is supported by CNPq (Brazil). F.M.P is supported by the Belgian National Science Foundation.

[1] A. Zrenner, F. Koch, J. Leotin, M. Goiran, and K. Ploog, Semicond. Sci. Technol. **3**, 1132 (1988).
[2] P.M. Koenraad, in *Delta Doping of Semiconductors*, edited by E.F. Schubert (Cambridge University Press, Cambridge, England, 1995).
[3] G.Q. Hai, N. Studart, F.M. Peeters, J.T. Devreese, P.M. Koenraad, A.F.W. van de Stadt, and J.H. Wolter, *Proceedings of the 22nd International Conference on the Physics of Semiconductors*, edited by J. Lockwood (World Scientific, Singapore, 1995).
[4] E.F. Schubert, J.E. Cunningham, and W.T. Tsang, Solid State Commun. **63**, 591 (1987); E.F. Schubert, J. Vac. Sci. Technol. A **87**, 2980 (1990).
[5] G. Gillman, B. Vinter, E. Barbier, and A. Tardella, Appl. Phys. Lett. **52**, 972 (1988).
[6] E. Skuras, R. Kumar, R.L. Williams, R.A. Stradling, J.E. Dmochowski, E.A. Johnson, A. Mackinnon, J.J. Harris, R.B. Beall, C. Skierbeszewski, J. Singleton, P.J. van der Wel, and P. Wisnieski, Semicond. Sci. Technol. **6**, 535 (1991).
[7] G.Q. Hai, N. Studart, and F.M. Peeters, Phys. Rev. B (to be published).
[8] G.Q. Hai and N. Studart, Phys. Rev. B **52**, R2245 (1995).
[9] R. Enderlein, L.M.R. Scolfaro, and J. R. Leite, Phys. Rev. B **50**, 18 312 (1994).
[10] X. Zheng, T.K. Carns, K.L. Wang, and B. Wu, Appl. Phys. Lett. **62**, 504 (1993).
[11] P.M. Koenraad, A.C.L. Heessels, F.A.P. Blom, J.A.A.J. Perenboom, and J.H. Wolter, Physica B **184**, 221 (1993).
[12] T.K. Carns, X. Zheng, and K.L. Wang, Appl. Phys. Lett. **62**, 3455 (1993).
[13] H.H. Radamson, M.R. Sardela, Jr., O. Nur, M. Willander, B.E. Sernelius, W.-X. Ni, and G.V. Hansson, Appl. Phys. Lett. **64**, 1842 (1994).
[14] S. Das Sarma and F. Stern, Phys. Rev. B **32**, 8442 (1985).
[15] L. Hedin and B.I. Lundqvist, J. Phys. C **4**, 2064 (1971).
[16] S. Mori and T. Ando, Phys. Rev. B **19**, 6433 (1979).
[17] J.K. Jain and S. Das Sarma, Phys. Rev. B **36**, 5949 (1987).
[18] R. Fletcher, E. Zaremba, M. D'Iorio, C.T. Foxon, and J.J. Harris, Phys. Rev. B **41**, 10 649 (1990).
[19] W. Xu, F.M. Peeters, and J. T. Devreese, Phys. Rev. B **48**, 1562 (1993).